Open access • Journal Article • DOI:10.1039/C7TA11338B

Water splitting to hydrogen over epitaxially grown InGaN nanowires on a metallic titanium/silicon template: reduced interfacial transfer resistance and improved stability to hydrogen — Source link

Mohamed Ebaid, Jung-Wook Min, Chao Zhao, Tien Khee Ng ...+2 more authors

Institutions: King Abdullah University of Science and Technology, SABIC

Published on: 24 Apr 2018 - Journal of Materials Chemistry (The Royal Society of Chemistry)

Topics: Water splitting, Hydrogen, Substrate (electronics), Nanowire and Epitaxy

Journal of
Materials Chemistry A

Accepted Manuscript

This article can be cited before page numbers have been issued, to do this please use: M. Ebaid, J. Min, C. Zhao, T. K. Ng, H. Idriss and B. S. Ooi, *J. Mater. Chem. A*, 2018, DOI: 10.1039/C7TA11338B.

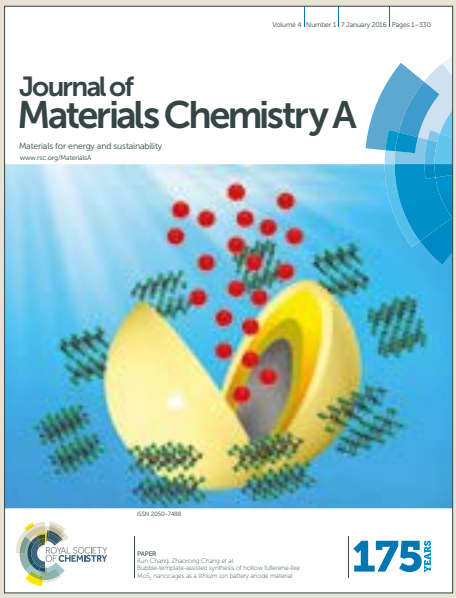

ROYAL SOCIETY OF CHEMISTRY

rsc.li/materials-a

View Article Online
DOI: 10.1039/C7TA11338B

Water Splitting to Hydrogen over Epitaxially Grown InGaN Nanowires on Metallic Titanium/Silicon Template: Reduced Interfacial Transfer Resistance and Improved Stability

Mohamed Ebaid[1], Jung-Wook Min[1], Chao Zhao[1], Tien Khee Ng[1], Hicham Idriss[2,*], and Boon S. Ooi[1,*]

[1]Photonics Laboratory, King Abdullah University of Science and Technology (KAUST), Thuwal 23955-6900, Saudi Arabia
[2]SABIC-Corporate Research and Development Center (CRD) at KAUST, Thuwal 23955, Saudi Arabia

*Email: boon.ooi@kaust.edu.sa and IdrissH@sabic.com

Water splitting using InGaN-based photocatalysts may have a great contribution in future renewable energy production systems. Among the most important parameters to solve are those related to substrate lattice-matching compatibility. Here, we directly grow InGaN nanowires (NWs) on a metallic Ti/Si template, for improving water splitting performance compared to a bare Si substrate. The open circuit potential of the epitaxially grown InGaN NWs on metallic Ti was almost two times more than when directly grown on Si substrate. The interfacial transfer resistance was also reduced significantly after introducing the metallic Ti interlayer. An applied-bias-photon-to-current conversion efficiency of 2.2% and almost unity Faradic efficiency for hydrogen generation were achieved using this approach. The InGaN NWs grown on Ti showed improved stability of hydrogen generation under continuous operation conditions, when compared to those grown on Si, emphasizing the role of the semiconductor-on-metal approach in enhancing the overall efficiency of water splitting devices.

View Article Online
DOI: 10.1039/C7TA11338B

Introduction

InGaN-based materials are recently attracting much attention due to their chemical stability and tunable band gap that can cover the entire visible solar spectrum and improve the solar light harvesting efficiency.[1] Several InGaN-based photoelectrolysis systems have already been demonstrated including single photoelectrodes[2-5], dual-photoelectrodes[6], and monolithic tandem cells.[7-9] However, the commercial applications of these structures are hindered by the low solar-to-hydrogen (STH) energy conversion efficiency, which is limited to values far from that achieved by III-V compound semiconductors such as GaInP/GaAs tandem cells.[10] This can be partially attributed to the lack of compatible and highly conductive substrates, which are indispensable for the efficient separation and transport of the photo-generated charge carriers to the desired water redox interfaces.[2] Motivated by the inert nature of wide bandgap and wide compositional tunability of group-III nitride, as well as the feasible single crystal growth of nitride-based nanowires (NWs) on scalable silicon substrate, we investigated the combination of both nitride NWs with silicon substrate in the presence of a metallic interlayer.

The growth of InGaN NWs usually involved single crystalline substrates, such as semi-insulating sapphire and semi-conducting Si. For instance, high aspect ratio InGaN NWs are typically grown by metalorganic chemical vapor deposition (MOCVD) on sapphire using metal catalyzed vapor-liquid-solid (VLS)[3] or selective area growth (SAG) techniques.[11] On the other hand, plasma-assisted molecular beam epitaxy (PA-MBE) has been dedicated for the growth of vertically-aligned InGaN NWs with high In-content on Si under nitrogen-rich conditions.[12] The prerequisite of growing InGaN NWs by PA-MBE under nitrogen rich conditions led, however, to the formation of inherent amorphous SiN_x insulating layers between the GaN/Si heterointerface.[13] The formation of the insulating SiN_x thin film was reported to increase the

View Article Online
DOI: 10.1039/C7TA11338B

interfacial resistance and introduce a large conduction band offset with n-GaN that can resist the charge carrier transport during the water splitting process.[14] Therefore, the growth of InGaN NWs on substrates made of conventional metals can provide new opportunities for enhancing the photo-generated charge carrier transport that can significantly improve the STH efficiency.

The potential of employing metallic substrates for the fabrication of photoelectrodes stems from the utilization of the high thermal and electrical conductivity and the potentially high optical reflectivity of metals as well as the freedom of enabling scale-up for field deployment.[15] The semiconductor-on-metal approach can play a vital role in the improvement of carrier extraction/collection efficiency that is crucial to accelerate the water redox reaction rates. Furthermore, metal substrates can act to mitigate the current crowding effects at the InGaN NWs/substrate interface leading to enhanced carrier collection and increased effective surface area for water splitting reactions.[16] The growth of III-V NWs on metallic substrates has already been demonstrated for the optoelectronic devices, which showed significant improvement of the device efficiency.[17-18] Although this approach can greatly contribute to improving the overall STH of water splitting, this concept was rarely reported.[2] This can be attributed to the difficulties of tuning the growth conditions to obtain high density of vertically aligned InGaN NWs.[15, 17]

In this study, we investigate the photoelectrochemical (PEC) performance of high quality InGaN NWs grown on a metallic Ti thin film deposited on Si substrates. Ti thin film was considered for integration with silicon substrate for both scalability and cost-effectiveness, ideal for future industrial uptake in both template-substrate production and PEC cell deployment. Here, the Si substrate was only used as a low-cost mechanical support for Ti thin film. The use of Ti carries the following advantages. It is well known that Ti-metal is a good Ohmic contact for n-type GaN,[19] and the electrical resistivity of Ti is approximately 4.2×10^{-5} Ohm.cm, which is much

View Article Online
DOI: 10.1039/C7TA11338B

lower than that of the commercial n-type Si (<0.01 Ohm.cm). Another key advantage is that, without a metal interlayer, an amorphous SiN_x dielectric thin film was known to have formed when InGaN NWs were directly grown on Si substrates. On the other hand, the Ti surface was reported to be partially nitrided due to the exposure of the surface to nitrogen plasma during the PA-MBE growth.[18] As compared to the insulating SiN_x, TiN exhibits a metallic conductivity and has a larger work function (4.25 eV) than that of the n-GaN (4.11 eV), which can help to extract the photo-generated electrons due to the reduced contact resistance and the favorable Ohmic heterointerface.[2, 15, 20]

The GaN/TiN/Ti interface was shown herein to improve the interfacial properties between the InGaN NWs and the electrolyte as verified using open circuit potential (OCP) measurements and Nyquist plots. The InGaN NWs on Ti showed improved PEC performance in terms of higher current densities, power conversion efficiencies, and the amount of evolved gases than those grown directly on Si-substrates. This investigation therefore contributes to communicating the unique treatment of interfacial properties of InGaN NWs/Si-substrate for effective extraction of minority carriers during PEC water splitting, and advancing the understanding of solar hydrogen generation using low cost platforms for eventual large-scale deployment.

Results and Discussion:

InGaN NWs were grown by PA-MBE on a metallic Ti-coated 2-inch Si (100) substrate and compared with those grown on bare Si (100) substrate. The silicon substrates were Sb-doped with a resistivity of <0.01 Ohm-cm. The thickness values of Ti were chosen to be 100, 200, and 300 nm, beyond which the thin films were found to exhibit severe cracks and rough surfaces. As shown by scanning electron microscopy (SEM) images in Fig. 1(a) and (b), the InGaN NWs

View Article Online
DOI: 10.1039/C7TA11338B

were vertically aligned on the Ti-surface with high density of > 10^{10} cm^{-2} and with uniform lengths of approximately 300 nm and lateral sizes of ~80-100 nm. As schematically shown in Fig. 1(c), the axial structure of the NWs is composed of small GaN seeds grown directly on the Ti film followed by InGaN NWs (details are given in the methodology section). Both GaN and InGaN layers were intentionally doped with Si-dopants to form n-type semiconductors. While there was no significant difference in the morphology of InGaN NWs grown on Ti or Si surfaces, the normalized photoluminescence (PL) spectra of InGaN NWs grown on Ti exhibited two main characteristics, as shown in Fig. 1(d). The PL spectra were blue shifted by approximately 0.14 eV for 100 and 200 nm Ti layer, while it was shifted by 0.25 eV with increasing the Ti thickness to 300 nm. Typically, the blue shift of the PL peak position of InGaN NWs is attributed to a reduced In composition.[1, 21-22] PL spectra of InGaN NWs grown on Ti revealed a narrower full-width at half-maximum (FWHM) than that of those grown directly on Si. Furthermore, InGaN NWs grown on 100 nm Ti showed a main peak centered at 585 nm with a weak shoulder peak at 550 nm. InGaN NWs grown on 200 and 300 nm thick Ti also exhibited PL peaks centered at almost the same positions, where the relative intensity of the two peaks increased with increasing the Ti thickness. The differences of the PL emissions of InGaN NWs grown on Ti could be originated from the higher thermal conductivity of the Ti metal as compared to that of Si.[22] The average In-content of InGaN NWs grown on 300 nm Ti was estimated from the PL spectra to be approximately 33% using Vegard's law, $E_g(x) = E_g(InN)x + E_g(GaN)(1-x) - Bx(1-x)$, with a bowing parameter (B) of 1.5 eV and GaN and InN bandgap energies of 3.4 and 0.7 eV, respectively.[1, 23-24] It is to be stressed that the average In composition does not guarantee a homogeneous solid solution and as per the shape of the luminesce spectra patches of InGaN of different In/Ga ratios are most likely present.

View Article Online
DOI: 10.1039/C7TA11338B

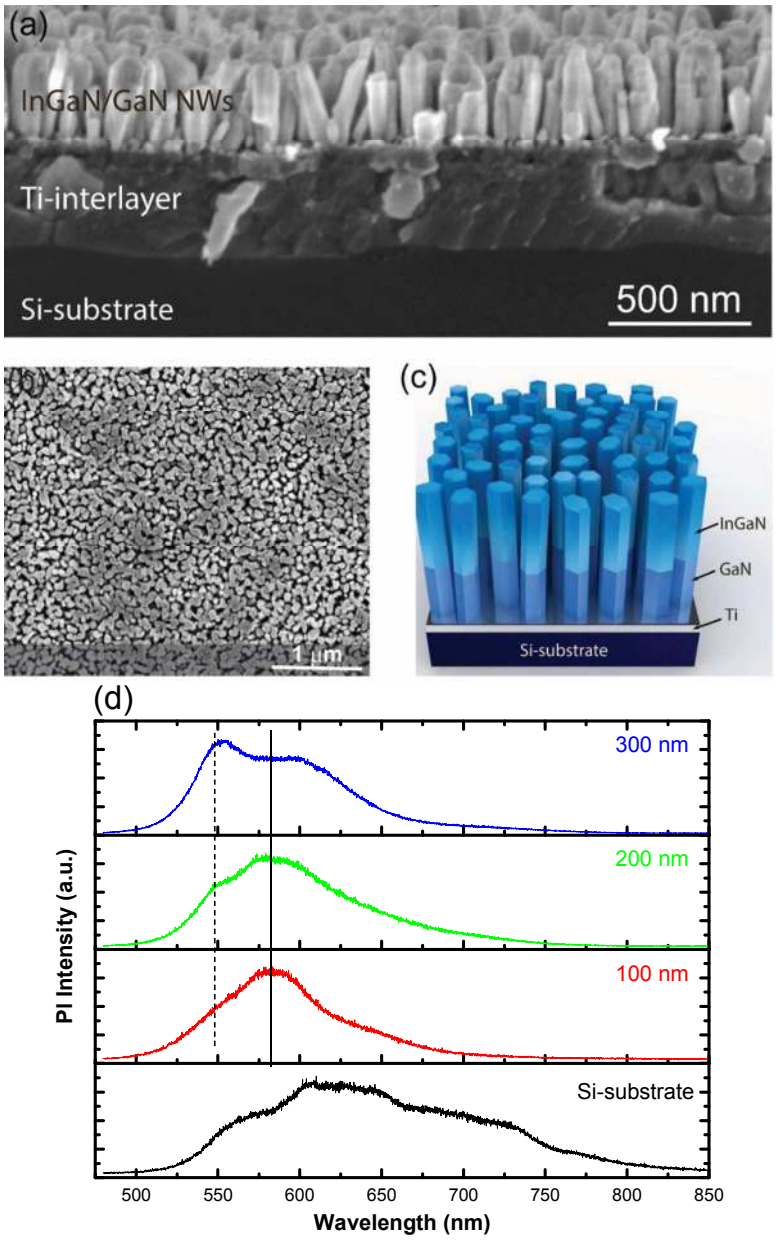

Figure 1: Morphology and optical properties of InGaN NWs. (a) Cross-sectional SEM image showing the morphology of the vertically-aligned InGaN NWs on a 300 nm Ti thin film/Si-substrate. (b) Plan-view SEM image showing the high density and uniform orientation of the InGaN NWs. (c) Schematic diagram showing the axial structure of the whole NW. (d) Normalized PL spectra of the InGaN NWs as a function of Ti-thickness, as compared to that of the bare Si-substrate measured at room temperature. The sold vertical line represent the center of the emission and the dashed vertical line is a guide to the eye of an emission at ca. 550nm.

View Article Online
DOI: 10.1039/C7TA11338B

To probe the interfacial properties of metallic Ti thin film after the temperature cycling during substrate outgassing and PA-MBE growth, we have investigated the atomic level details of the interface by high-resolution transmission electron microscopy (HR-TEM), electron energy loss spectroscopy (EELS), and fast Fourier transform (FFT) imaging techniques. HR-TEM images shown in Fig. 2(a) and (b) revealed the high crystal quality of the grown InGaN NWs regardless of the bottom surface. Due to the exposure of the surface to nitrogen plasma, thin interfacial layers were formed during the early growth steps on both Si and Ti surfaces. These interfacial layers can be identified from the HR-TEM and EELS mapping to be approximately 3.5 nm of amorphous SiN_x and 1 nm of crystalline TiN for the bare Si-substrate and the Ti-coated Si-substrate, respectively. The interfacial layer formed between GaN and Ti was further investigated by FFT imaging, confirming the existence of a face centered cubic TiN with a lattice spacing of 2.45 Å and establishing the epitaxial relation of (0002)GaN // (111)TiN.[18] No inter-diffusion between Ti and the InGaN NWs was observed. The corresponding energy band diagram of the InGaN NWs on Si and Ti are schematically shown in Fig. 2 (e) and (f), respectively. During the PEC water splitting process, as the n-type InGaN NWs are brought into contact with the electrolyte and under light conditions, there will be an upward band bending due to the transport of the excess charge carriers from the semiconductor NWs to the electrolyte to achieve the electrochemical equilibrium. The photo-generated holes will then diffuse to the InGaN NWs/electrolyte interface to start the water oxidation reaction and the photo-generated electrons will migrate towards the bottom n-GaN to the counter electrode to reduce hydrogen ions into hydrogen molecules. The small conduction band offset between n-InGaN and n-GaN will allow electrons to readily tunnel through, while the transport of holes in the same direction will be hindered by the large valence band offset, which will help in charge separation. To

View Article Online
DOI: 10.1039/C7TA11338B

accelerate the water oxidation step, metal ions co-catalysts are typically deposited on the surface of InGaN NWs to extract the photo-generated holes.[2, 4, 25] On the other hand, for the photo-generated electrons to be easily transported to the counter electrode and start the hydrogen reduction an Ohmic contact is needed. In the case of InGaN NWs grown on Si, due to the large conduction band offset between the GaN and the insulating SiN_x thin film, the transportation of the photo-generated electrons is challenging and consequently the reaction may not occur. On the other hand, the Ohmic contact formed by the TiN/Ti metal stack is beneficial for electron transport due to a comparable work functions of TiN (4.25 eV)[26]and Ti (4.3 eV)[27]to that of n-type GaN (4.1 eV).[28] The PEC performance of the InGaN NWs on Ti and Si is discussed in the following paragraphs.

View Article Online
DOI: 10.1039/C7TA11338B

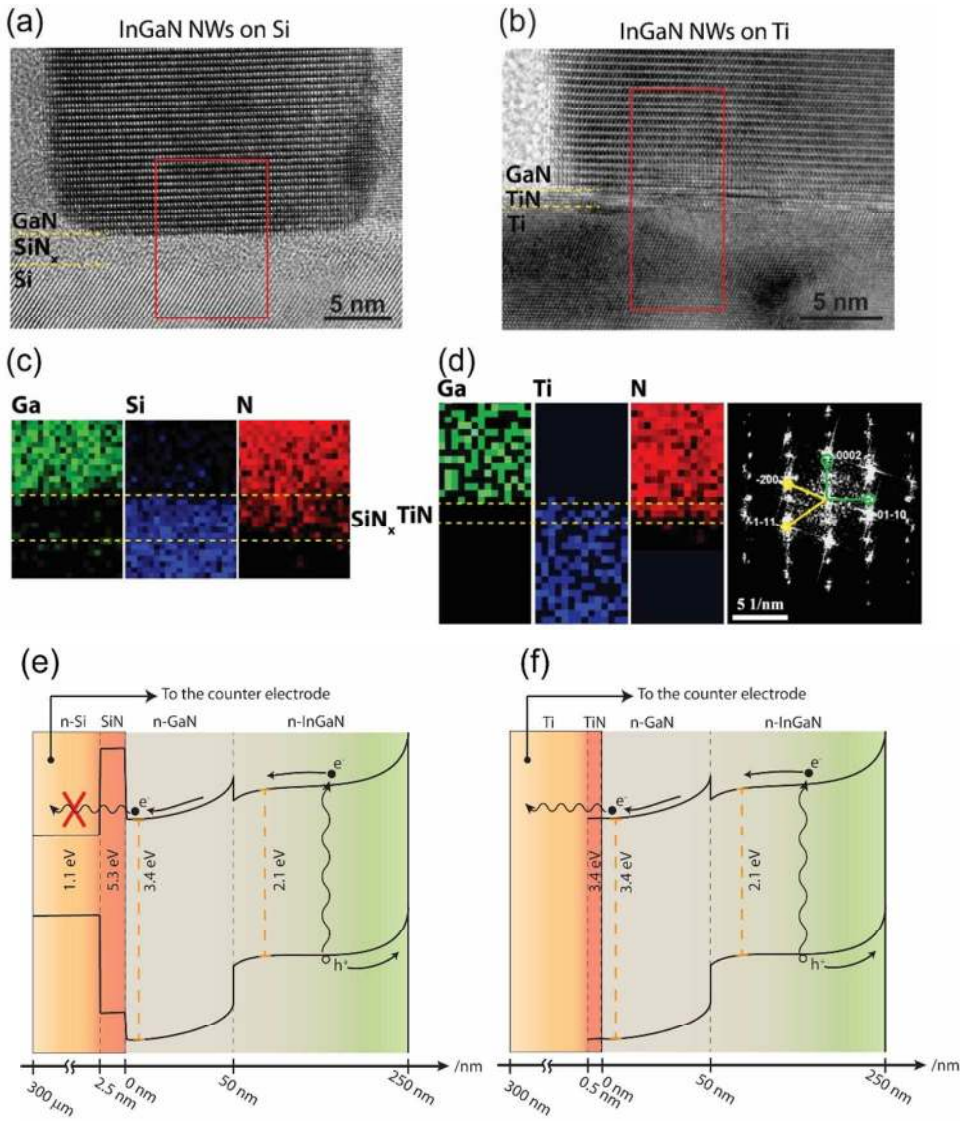

Figure 2: Interfacial properties of InGaN NWs on Ti and Si surfaces. (a) and (b) cross-sectional HR-TEM images showing the GaN/SiN_x/Si and GaN/TiN/Ti heterointerfaces. (c) and (d) the corresponding EELS mappings of the same heterointerfaces. The FFT image of the GaN/TiN interface is also shown in panel (d). (e) and (f) Schematic representations of the energy band diagram of the InGaN NWs on Si and Ti surfaces, respectively.

To ascertain the Ti metal effect on charge carrier diffusion, we have investigated the open-circuit potential (OCP) of the samples in the dark and under illumination conditions, as depicted in Fig. 3(a). From the shift of the OCP under illumination one can extract information about the type of conductivity as well as its associated photovoltage. For example, as an n-type

View Article Online
DOI: 10.1039/C7TA11338B

semiconductor is brought into contact with an electrolyte under dark conductions, an upward band-bending of the surface energy bands occurs at equilibrium due to excess charge carrier transport from the semiconductor to the electrolyte at the interface. Upon illumination with sufficient light intensity, the photo-generated free minority carriers (holes) induce an upward shift in the surface quasi-Fermi level of the majority carriers (electrons) thereby flattening the bands, leading to a negative shift in the OCP. As shown in Fig. 3(a), upon illumination all samples showed a rapid decrease in the OCP, which slowly increases again as light is switched off, indicating an n-type conductivity and anodic PEC behavior.[29] The negative shift of the illuminated OCP values increased linearly with increasing the Ti-thickness, reaching -150 mV vs RHE at 300 nm of Ti, which is much larger than the bare Si-substrate. In principle, the difference between the OCP in the dark and under illumination represents the photovoltage caused by the potential difference within the space charge region in the semiconductor resulting from surface Fermi level pinning.[29] The effective transport of the photo-generated charge carriers in the InGaN NWs grown on Ti as evident in the significant change in OCP (~500 mV vs RHE), is about two times that of the Si-substrate (~270 mV vs RHE).

Electrochemical impedance spectroscopy (EIS) was further used to elucidate the interfacial charge transport kinetics under light illumination. As shown in the proposed model schematically represented in Fig. 3(b), the EIS data are fitted by assuming an R(RC) model (Randles circuit) consisting of a series resistance (R_s) associated with the semiconductor photoanode and the Ohmic contacts, a hole transfer resistance (R_{ct}) from the valence band of the semiconductor to the electrolyte, and a constant phase element (CPE) represents the double-layer capacitance. Figures 3(c) and (d) display the Nyquist plots representing the internal resistances corresponding to the overall charge transfer process with respect to the applied frequency. The

View Article Online
DOI: 10.1039/C7TA11338B

semicircle at high frequency in a Nyquist plot represents the charge transfer at the InGaN NWs/electrolyte interface while its diameter is equivalent to the charge transfer resistance.[30] The InGaN NWs on Ti and those on the bare Si-substrate have different responses. The InGaN NWs grown on Si-substrate exhibited much larger charge transfer resistance than those grown on Ti. Furthermore, the impedance profile measured for the InGaN NWs grown on Si-substrate is characterized by two semicircles, one at high frequency (fast response) and another dominant one at low frequency (slow response) indicating an additional resistance to the charge carrier transport. As shown in the inset of Fig. 3(c), the equivalent circuit used to fit the impedance data of the InGaN NWs grown on Si-substrate consists of two RC elements connected in series referring to the existence of two different resistances, which can be attributed to the interfacial SiN_x and the bulk Si-substrate itself. In the case of InGaN NWs on Ti, the impedance results were well fitted with the Randles circuit having only one RC element representing one interfacial resistance, which is very small compared to that of the bare Si-substrate. Based on the results shown by OCP and Nyquist plots, we can conclude that the growth of semiconductor NWs on a metallic substrate reduces the interfacial charge transport resistance, which is poised to enhance the water splitting reaction.

View Article Online
DOI: 10.1039/C7TA11338B

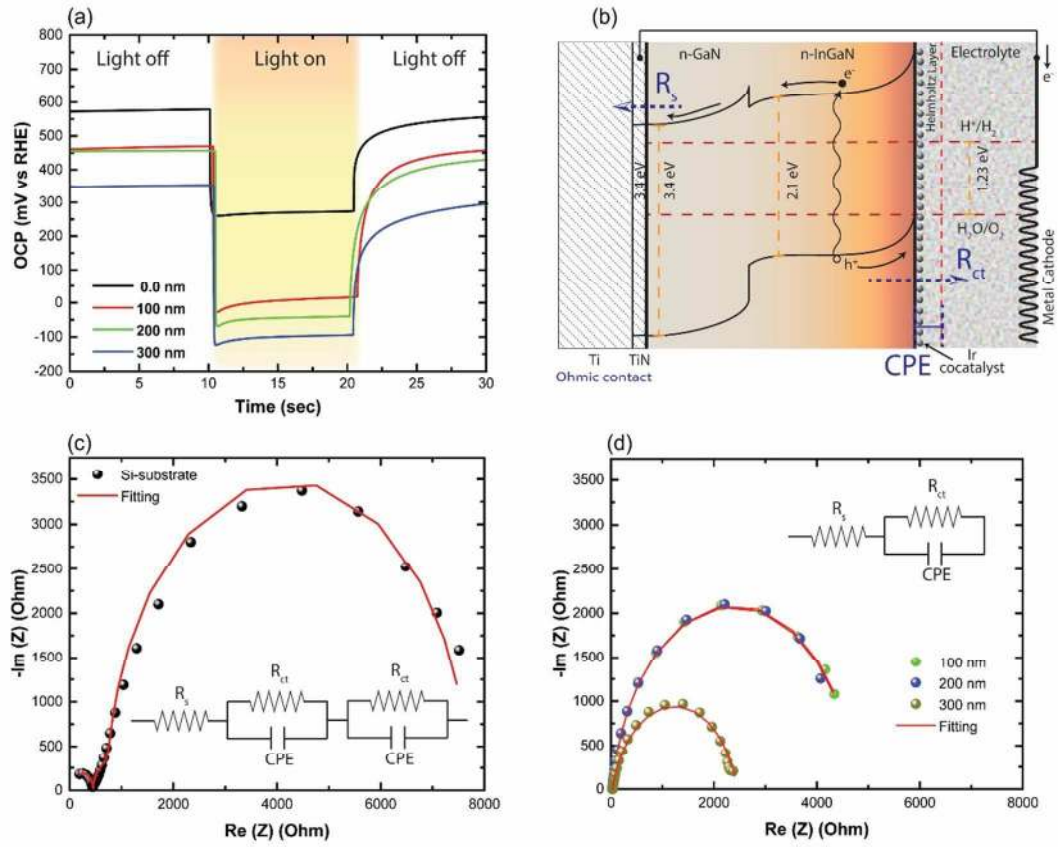

Figure 3: OCP and Nyquist plots of InGaN NWs grown on Ti as compared to those on Si. (a) OCP under dark and light conditions. (b) Schematic diagram of the proposed R(RC) Randles model used in the impedance analysis. (c) and (d) show the Nyquist plots of the InGaN NWs on Si and Ti/Si substrates, respectively.

The influence of using a metallic Ti-interlayer as a charge extraction/collection layer was further investigated by measuring the response of the InGaN NWs photoanodes to the applied potential. Linear scan voltammetry (LSV) was subsequently performed in a three-electrode PEC cell with a Pt-mesh as the counter electrode and Ag/AgCl as the reference electrode under dark and light conditions. The applied potential was converted relative to RHE using the equation $E_{(RHE)} = E^{\circ}_{(Ag/AgCl)} + E_{(Ag/AgCl)} + 0.059 \times pH$ where, $E_{(Ag/AgCl)}$ is the potential of the Ag/AgCl electrode, and $E^{\circ}_{(Ag/AgCl)}$ is the standard potential of the Ag/AgCl electrode (0.197 V). A highly conductive metallic wire was directly attached to the top of the Ti-interlayer, as shown

View Article Online
DOI: 10.1039/C7TA11338B

in the inset of Fig. 4(a), to exclude any contribution from the Si-substrate. To reduce the overpotential and for efficient separation and extraction of the photo-generated holes at the InGaN/electrolyte interface, Ir-metal nanoparticles were deposited on the surface of InGaN NWs by dip coating (see Fig. 4(a) for the sample without Ir co-catalyst)). Negligible dark currents were observed for all samples. Mass-transport-limited anodic current density of approximately 2 mA/cm^2 was observed for the InGaN NWs grown on 300 nm thick Ti-interlayer with a cathodic shift of the onset potential to approximately -0.1 V vs RHE which is matching with that estimated from Fig. 3(a). For comparison, the InGaN NWs grown on the bare Si-substrate showed a linear increase of the current density with the applied potential without reaching the potential independent regime even at 1.6 V vs RHE. The small current density measured for the InGaN NWs photoanode fabricated directly on the bare Si-substrate can be a result of the low conductivity (compared to that of the Ti/Si template) and the large conduction band offset introduced by the formation of insulating SiN_x that can oppose the electron transport to the counter electrode. On the other hand, the PEC performance of the InGaN NWs photoanodes fabricated on Ti was dramatically improved as seen by the rapid saturation of the current density and the large cathodic shift of the onset potential. This can be attributed to the improved carrier extraction/collection efficiency due to the reduced interfacial resistance (Fig. 3) and the faster charge carrier transport to the desired water redox interfaces.

The applied-bias-photon-to-current conversion efficiency (ABPE) was used to evaluate the performance of the photoanodes with respect to the applied potential, as shown in Fig. 4(b). This is given by $ABPE(\%)=100\times J(mA/cm^2)(1.23-V_{app})/P_{light}(mW/cm^2)$,[2] where J is the current density, 1.23 V is the standard-state reversible potential of the water, V_{app} is the applied potential, and P_{light} is the light power density. The InGaN NWs grown on Ti achieved an ABPE

View Article Online
DOI: 10.1039/C7TA11338B

of 2.2% at almost 0.61 V vs RHE compared to only 0.2% at 1.1 V vs RHE for those grown on Si-substrate. Hence, about 12 times increase in power conversion efficiency was achieved by using a metallic Ti as a charge extraction/collection interlayer. To gain insight on the number of absorbed photons converted into photogenerated charge carriers, the incident-photon-to-current efficiency (IPCE) was measured as a function of monochromatic light irradiation. The static current density was measured as the difference between dark and illumination conditions using chronoamperometry (CA) technique, and the IPCE values are derived at fixed applied bias of 0.85 V vs RHE (close to the optimum working potential obtained from the ABPE) using the following equation: $IPCE(\%) = 100 \times 1240(V.nm) \times J\ (mA.cm^{-2})/\lambda(nm) \times P_{\text{light}}(mW.cm^{-2})$. As shown in the inset of Fig. 4(b), the IPCE of the InGaN NWs grown on Si-substrate was significantly improved after using a 300 nm of metallic Ti interlayer, which can be attributed to the enhanced charge extraction/collection efficiency (current density).

An important criterion for the development of PEC cell for hydrogen generation for eventual deployment is the issue of reliability. The stability of the InGaN NWs on Ti as well as on Si was therefore investigated using CA in neutral solution (pH~7) under AM1.5G irradiation and with the previously applied bias of 0.85 V vs RHE. The InGaN NWs grown on the bare Si-substrate exhibited a very small current density, which almost vanished within the first hour of the experiment. This kind of stability degradation was partially attributed to the formation of SiN_x at the GaN/Si heterointerface, which was reported to be rapidly etched during the water splitting process leading to associated GaN etching as well as increased interfacial resistance.[7] On the other hand, when the same InGaN NWs were fabricated on Ti, the current density increased with time before it reach a plateau after approximately one hour. The inset of Fig. 4(c)

View Article Online
DOI: 10.1039/C7TA11338B

shows the difference between the current density measured after almost three hours of continuous irradiation under light and dark conditions indicating a good photoactivity of the photoanode. The InGaN NWs on Ti exhibited a stable current density of approximately 1 mA/cm^2 after continuous illumination of 5 hours.

The amount of the evolved hydrogen and oxygen gases during the stability test were then measured using gas chromatography for the InGaN NWs grown on 300 nm Ti sample. As shown in Fig. 4(d), hydrogen and oxygen gases linearly increased with time with a molar ratio close to 2:1 indicating a good extraction/collection efficiency of the photo-generated charge carriers. The Faradic efficiency was calculated using the equation $\eta_{Faraday} = 2 \times n_{H_2}(\mu mol) \times F \Big/ \int_0^t I(mA).dt$,[7] where n_{H_2} is the total amount of hydrogen produced (μmol) with time (t), F is the Faradic constant (96485 C/mol), and I is the current in mA. The Faradic efficiency was calculated to be 96.6 %, which can be observed as the matching between the measured and the calculated amount of hydrogen gas. By considering the error of the gas sampling (~5%) and analysis, it is possible to assume that the Faradic efficiency is unity, which emphasis the impact of the semiconductor-on-metal approach on the enhanced PEC water splitting performance.

View Article Online
DOI: 10.1039/C7TA11338B

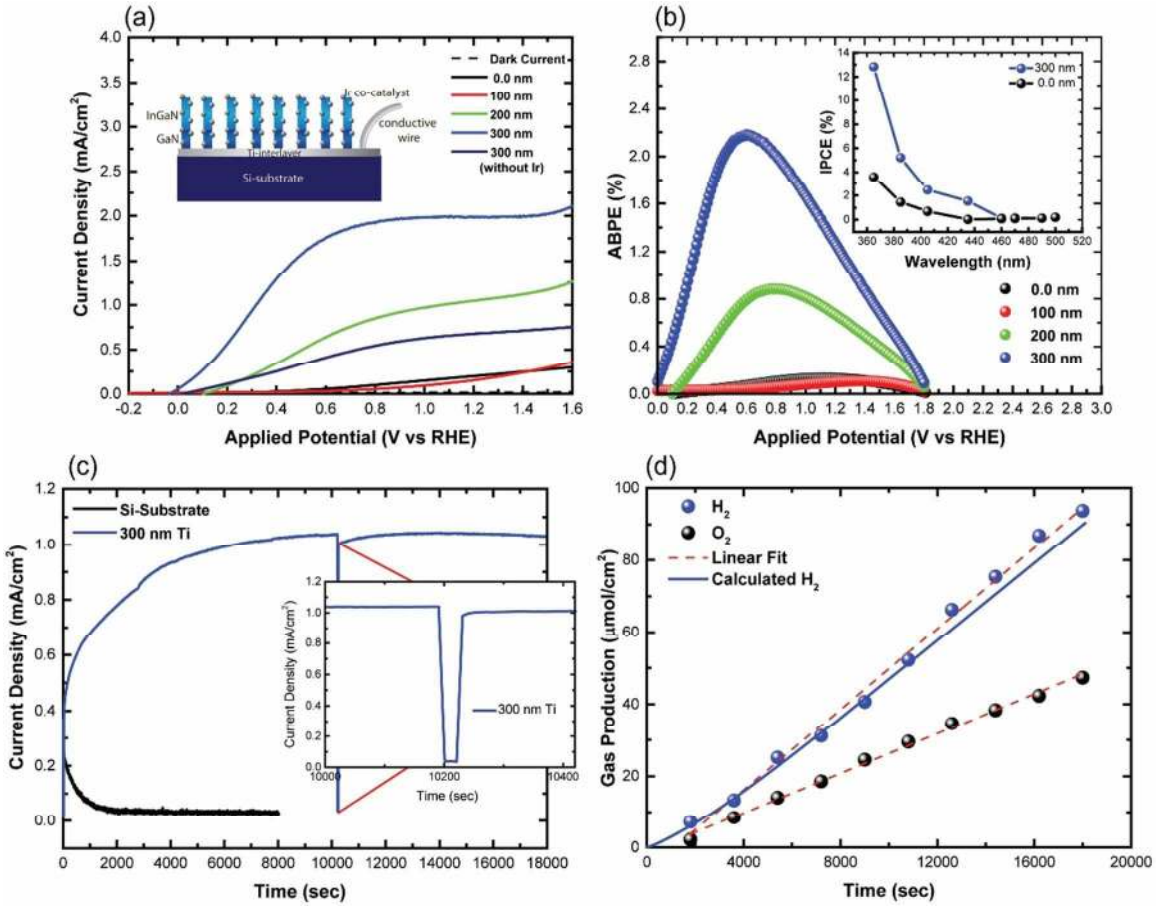

Figure 4: PEC performance of InGaN NWs grown on Ti as compared to those on Si. (a) LSV of InGaN NWs under dark and light conditions. (b) ABPE of InGaN NWs as a function of Ti-thickness. Inset is the IPCE of InGaN NWs grown on 300 nm Ti as compared to those grown directly on Si. (C) Chronoamperometric test of the InGaN NWs on Ti and Si. (d) The gas evolution measured during the chronoamperometric test shown in (C). The light intensity was fixed at approximately 500 mW/cm^2 during all the PEC measurements.

Conclusions

In conclusion, the growth of InGaN NWs on the conventional Si-substrates showed a poor PEC performance in terms of a low current density and degradation of the photoanode with time, which can be attributed to the formation of the amorphous insulating SiN_x interfacial films and the associate effect on charge transport resistance during the water splitting process. By addressing the issues of instability of InGaN NWs on Si substrates we have concluded that it is

View Article Online
DOI: 10.1039/C7TA11338B

linked to the presence of a layer of SiN_x at the interface which blocked excited carrier diffusion due to its high band gap energy. We have then succeeded in putting a Ti layer in between the Si substrate and InGaN NWs. A 300 nm Ti layer was found to be adequate to increase charge carriers' concentration and resolve the SiN_x formation. An improved charge carrier extraction/collection efficiency and a reduced interfacial resistance were noticed for all Ti layers. The InGaN NWs on Ti could also retain the same initial current density after continuous illumination for 5 hours and continuously produce hydrogen and oxygen gases with a Faradic efficiency close to unity.

Acknowledgments

We acknowledge financial support from Saudi Basic Industries Corporation (SABIC), Grant No. RGC/3/3068-01-01. BSO, TKN, CZ, and JWM acknowledge funding from King Abdulaziz City for Science and Technology (KACST), Grant No. KACST TIC R2-FP-008. This work was partially supported by King Abdullah University of Science and Technology (KAUST) baseline funding, BAS/1/1614-01-01.

Methodology

The InGaN NWs were grown on a bare Si-substrate and Ti coated 2-inch Si (100) substrate using VEECO GEN 930 PA-MBE. Before growth or Ti deposition, Si-substrates were chemically cleaned to remove the native oxide. Prior to the growth of InGaN, GaN seeds were first grown for 30 min with Ga and N are the only used precursors. Immediately after the growth of GaN seeds, In was introduced to the PA-MBE chamber and the growth of InGaN was started and lasted for 2 hours. The InGaN NWs were grown with Ga and In beam equivalent pressures of 3 to 6×10^{-8} and 5×10^{-8} Torr, respectively. The nitrogen plasma power was maintained at 350 W with 1 sccm during the whole growth. The morphology of the InGaN NWs was characterized

View Article Online
DOI: 10.1039/C7TA11338B

using Quanta 3D FEG field emission scanning electron microscopy (SEM) working at 5 kV. To study the interfacial properties at the GaN/Si and GaN/Ti heterointerfaces, a cross-sectional TEM FEI Titan 80–300 kV (ST) with a field-emission gun operating at 300 kV was employed. The TEM was equipped with an EDS Genesis apparatus coupled to the FEI Quanta 600FEG SEM energy dispersive X-ray spectroscopy (EDS) detector.

Prior to the attachment of Ir nanoparticle co-catalysts, the surface native oxides of the InGaN NWs were removed at room temperature by buffered oxide etch (BOE) for 30 sec followed by ethanol cleaning and then dipping in 1 mg/mol $IrCl_3$ dissolved in 5:1 CH_3CN:H_2O for 30 min. The PEC experiments were conducted in a three-electrode configuration cell using InGaN NWs as the working electrode, Ag/AgCl as the reference electrode, and a Pt-mesh as the counter electrode. A 0.1M potassium phosphate buffer solution (pH~7) was used as the electrolyte. The photoanodes were irradiated with simulated sunlight produced by an AM1.5G filter using the solar simulator HAL-320, Asahi Spectra. The LSV (scan rate was 10 mV/sec) and chronoamperometry tests were performed using a single channel potentiostat PARSTAT4000+ controlled by VersaStudio software. The IPCE was measured using a CoolLED (pE-4000) light source, where the power density of the monochromatic light was measured using Newport power meter (2936-C) connected to a Newport 818-UV calibrated detector. The PEC cell was placed inside a black enclosure to avoid the background light. Gas evolution by water splitting was performed in a leak-tight glass reactor with a quartz window connected to a closed gas circulation which was purged by high purity nitrogen before illumination. The total volume of the reactor was 160 ml and the InGaN NWs photocatalyst was immersed in 100 mL of 0.1M potassium phosphate buffer solution (pH~7). The evolved gases during the water splitting experiment were collected and quantified using two separate gas chromatographs (GCs) SRI

View Article Online
DOI: 10.1039/C7TA11338B

310c. In the case of hydrogen gas, a HayeSep Q column and a nitrogen carrier gas were used, while a molecular sieve (5A) column, with a helium carrier gas, was used for the oxygen gas measurements. The two GCs were calibrated for hydrogen and oxygen gases and the slope of the calibration curve was used to calculate the number of moles by considering the peak area for each gas sample. The total number of moles was then calculated by multiplying the last value by the reactor head space (60 ml), which was normalized to the surface area of the InGaN NWs photocatalyst.

References:

1. Kuykendall, T.; Ulrich, P.; Aloni, S.; Yang, P., Complete composition tunability of InGaN nanowires using a combinatorial approach. *Nat Mater* **2007,** *6* (12), 951-956.
2. Ebaid, M.; Priante, D.; Liu, G.; Zhao, C.; Sharizal Alias, M.; Buttner, U.; Khee Ng, T.; Taylor Isimjan, T.; Idriss, H.; Ooi, B. S., Unbiased photocatalytic hydrogen generation from pure water on stable Ir-treated In0.33Ga0.67N nanorods. *Nano Energy* **2017,** *37*, 158-167.
3. Ebaid, M.; Kang, J.-H.; Lim, S.-H.; Ha, J.-S.; Lee, J. K.; Cho, Y.-H.; Ryu, S.-W., Enhanced solar hydrogen generation of high density, high aspect ratio, coaxial InGaN/GaN multi-quantum well nanowires. *Nano Energy* **2015,** *12*, 215-223.
4. Varadhan, P.; Fu, H.-C.; Priante, D.; Retamal, J. R. D.; Zhao, C.; Ebaid, M.; Ng, T. K.; Ajia, I.; Mitra, S.; Roqan, I. S.; Ooi, B. S.; He, J.-H., Surface Passivation of GaN Nanowires for Enhanced Photoelectrochemical Water-Splitting. *Nano Letters* **2017,** *17* (3), 1520-1528.
5. Ebaid, M.; Kang, J.-H.; Lim, S.-H.; Cho, Y.-H.; Ryu, S.-W., Towards highly efficient photoanodes: the role of carrier dynamics on the photoelectrochemical performance of InGaN/GaN multiple quantum well coaxial nanowires. *RSC Advances* **2015,** *5* (30), 23303-23310.
6. AlOtaibi, B.; Fan, S.; Vanka, S.; Kibria, M. G.; Mi, Z., A Metal-Nitride Nanowire Dual-Photoelectrode Device for Unassisted Solar-to-Hydrogen Conversion under Parallel Illumination. *Nano Letters* **2015,** *15* (10), 6821-6828.
7. Fan, S.; AlOtaibi, B.; Woo, S. Y.; Wang, Y.; Botton, G. A.; Mi, Z., High Efficiency Solar-to-Hydrogen Conversion on a Monolithically Integrated InGaN/GaN/Si Adaptive Tunnel Junction Photocathode. *Nano Letters* **2015,** *15* (4), 2721-2726.
8. Dahal, R.; Pantha, B. N.; Li, J.; Lin, J. Y.; Jiang, H. X., Realizing InGaN monolithic solar-photoelectrochemical cells for artificial photosynthesis. *Applied Physics Letters* **2014,** *104* (14), 143901.
9. Fan, S.; Shih, I.; Mi, Z., A Monolithically Integrated InGaN Nanowire/Si Tandem Photoanode Approaching the Ideal Bandgap Configuration of 1.75/1.13 eV. *Advanced Energy Materials* **2017,** *7* (2), n/a-n/a.
10. May, M. M.; Lewerenz, H.-J.; Lackner, D.; Dimroth, F.; Hannappel, T., Efficient direct solar-to-hydrogen conversion by in situ interface transformation of a tandem structure. **2015,** *6*, 8286.

View Article Online
DOI: 10.1039/C7TA11338B

11. Bergbauer, W.; Strassburg, M.; Ch, K.; Linder, N.; Roder, C.; Lähnemann, J.; Trampert, A.; Fündling, S.; Li, S. F.; Wehmann, H. H.; Waag, A., Continuous-flux MOVPE growth of position-controlled N-face GaN nanorods and embedded InGaN quantum wells. *Nanotechnology* **2010,** *21* (30), 305201.
12. Goodman, K. D.; Protasenko, V. V.; Verma, J.; Kosel, T. H.; Xing, H. G.; Jena, D., Green luminescence of InGaN nanowires grown on silicon substrates by molecular beam epitaxy. *Journal of Applied Physics* **2011,** *109* (8), 084336.
13. Shetty, S.; Kesaria, M.; Ghatak, J.; Shivaprasad, S. M., The Origin of Shape, Orientation, and Structure of Spontaneously Formed Wurtzite GaN Nanorods on Cubic Si(001) Surface. *Crystal Growth & Design* **2013,** *13* (6), 2407-2412.
14. Basanta, R.; Mahesh, K.; Mohana, K. R.; Thirumaleshwara, N. B.; Krupanidhi, S. B., Binary group III-nitride based heterostructures: band offsets and transport properties. *Journal of Physics D: Applied Physics* **2015,** *48* (42), 423001.
15. Wölz, M.; Hauswald, C.; Flissikowski, T.; Gotschke, T.; Fernández-Garrido, S.; Brandt, O.; Grahn, H. T.; Geelhaar, L.; Riechert, H., Epitaxial Growth of GaN Nanowires with High Structural Perfection on a Metallic TiN Film. *Nano Letters* **2015,** *15* (6), 3743-3747.
16. Waki, I.; Cohen, D.; Lal, R.; Mishra, U.; DenBaars, S. P.; Nakamura, S., Direct water photoelectrolysis with patterned n-GaN. *Applied Physics Letters* **2007,** *91* (9), 093519.
17. Sarwar, A. T. M. G.; Carnevale, S. D.; Yang, F.; Kent, T. F.; Jamison, J. J.; McComb, D. W.; Myers, R. C., Semiconductor Nanowire Light-Emitting Diodes Grown on Metal: A Direction Toward Large-Scale Fabrication of Nanowire Devices. *Small* **2015,** *11* (40), 5402-5408.
18. Zhao, C.; Ng, T. K.; Wei, N.; Prabaswara, A.; Alias, M. S.; Janjua, B.; Shen, C.; Ooi, B. S., Facile Formation of High-Quality InGaN/GaN Quantum-Disks-in-Nanowires on Bulk-Metal Substrates for High-Power Light-Emitters. *Nano Letters* **2016,** *16* (2), 1056-1063.
19. Luther, B. P.; Mohney, S. E.; Jackson, T. N.; Asif Khan, M.; Chen, Q.; Yang, J. W., Investigation of the mechanism for Ohmic contact formation in Al and Ti/Al contacts to n-type GaN. *Applied Physics Letters* **1997,** *70* (1), 57-59.
20. Patsalas, P.; Kalfagiannis, N.; Kassavetis, S., Optical Properties and Plasmonic Performance of Titanium Nitride. *Materials* **2015,** *8* (6).
21. Ebaid, M.; Kang, J.-H.; Yoo, Y.-S.; Lim, S.-H.; Cho, Y.-H.; Ryu, S.-W., Vertically aligned InGaN nanowires with engineered axial In composition for highly efficient visible light emission. *Scientific Reports* **2015,** *5*, 17003.
22. Kucukgok, B.; Wu, X.; Wang, X.; Liu, Z.; Ferguson, I. T.; Lu, N., The structural properties of InGaN alloys and the interdependence on the thermoelectric behavior. *AIP Advances* **2016,** *6* (2), 025305.
23. Orsal, G.; El Gmili, Y.; Fressengeas, N.; Streque, J.; Djerboub, R.; Moudakir, T.; Sundaram, S.; Ougazzaden, A.; Salvestrini, J. P., Bandgap energy bowing parameter of strained and relaxed InGaN layers. *Opt. Mater. Express* **2014,** *4* (5), 1030-1041.
24. Juodkazytė, J.; Šebeka, B.; Savickaja, I.; Kadys, A.; Jelmakas, E.; Grinys, T.; Juodkazis, S.; Juodkazis, K.; Malinauskas, T., InxGa1−xN performance as a band-gap-tunable photo-electrode in acidic and basic solutions. *Solar Energy Materials and Solar Cells* **2014,** *130*, 36-41.
25. Ran, J.; Zhang, J.; Yu, J.; Jaroniec, M.; Qiao, S. Z., Earth-abundant cocatalysts for semiconductor-based photocatalytic water splitting. *Chemical Society Reviews* **2014,** *43* (22), 7787-7812.

View Article Online
DOI: 10.1039/C7TA11338B

26. Lima, L. P. B.; Diniz, J. A.; Doi, I.; Godoy Fo, J., Titanium nitride as electrode for MOS technology and Schottky diode: Alternative extraction method of titanium nitride work function. *Microelectronic Engineering* **2012,** *92* (Supplement C), 86-90.
27. Baca, A. G.; Ren, F.; Zolper, J. C.; Briggs, R. D.; Pearton, S. J., A survey of ohmic contacts to III-V compound semiconductors. *Thin Solid Films* **1997,** *308-309* (Supplement C), 599-606.
28. Bae, C.; Krug, C.; Lucovsky, G.; Chakraborty, A.; Mishra, U., Work-function difference between Al and n-GaN from Al-gated n-GaN/nitrided-thin-Ga2O3/SiO2 metal oxide semiconductor structures. *Applied Physics Letters* **2004,** *84* (26), 5413-5415.
29. Kamimura, J.; Bogdanoff, P.; Ramsteiner, M.; Corfdir, P.; Feix, F.; Geelhaar, L.; Riechert, H., p-Type Doping of GaN Nanowires Characterized by Photoelectrochemical Measurements. *Nano Letters* **2017,** *17* (3), 1529-1537.
30. Zhang, Z.; Wang, P., Highly stable copper oxide composite as an effective photocathode for water splitting via a facile electrochemical synthesis strategy. *Journal of Materials Chemistry* **2012,** *22* (6), 2456-2464.

View Article Online
DOI: 10.1039/C7TA11338B

1

2

View Article Online
DOI: 10.1039/C7TA11338B

Table of Contents

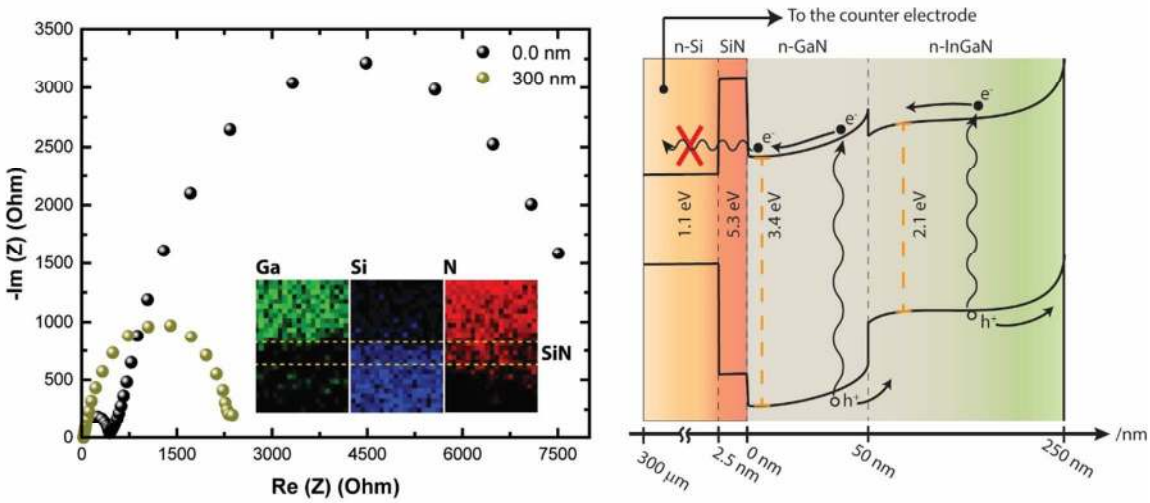

InGaN NWs were grown on a metallic Ti/Si template that improved the photoelectrochemical performance, stability, and reduced the interfacial transfer resistance